HHS Public Access

Author manuscript

Lasers Surg Med. Author manuscript; available in PMC 2015 June 18.

Published in final edited form as:

Lasers Surg Med. 2013 October ; 45(8): 533–541. doi:10.1002/lsm.22159.

High Contrast Reflectance Imaging of Simulated Lesions on Tooth Occlusal Surfaces at Near-IR Wavelengths

William A. Fried, **Daniel Fried, PhD**, **Kenneth H. Chan**, and **Cynthia L. Darling, PhD***

University of California, San Francisco, San Francisco, California, 94143-0758

Abstract

Introduction—In vivo and in vitro studies have shown that high contrast images of tooth demineralization can be acquired in the near-infrared (near-IR) without the interference of stain. The purpose of this study is to compare the lesion contrast in reflectance at near-IR wavelengths coincident with high water absorption with those in the visible, the near-IR at 1,300 nm and with fluorescence measurements for early lesions in occlusal surfaces.

Methods—Twenty-four human molars were used in this *in vitro* study. Teeth were painted with an acid-resistant varnish, leaving a 4 × 4 mm window in the occlusal surface of each tooth exposed for demineralization. Artificial lesions were produced in the exposed windows after 1- and 2-day exposure to a demineralizing solution at pH 4.5. Lesions were imaged using near-IR reflectance at three wavelengths, 1,300, 1,460, and 1,600 nm using a high definition InGaAs camera. Visible light reflectance, and fluorescence with 405 nm excitation and detection at wavelengths greater than 500 nm were also used to acquire images for comparison. Crossed polarizers were used for reflectance measurements to reduce interference from specular reflectance.

Results—The contrast of both the 1- and 2-day lesions were significantly higher ($P < 0.05$) for near-IR reflectance imaging at 1,460 and 1,600 nm than it was for near-IR reflectance imaging at 1,300 nm, visible reflectance imaging, and fluorescence.

Conclusion—The markedly higher contrast at 1,460 and 1,600 nm wavelengths, coincident with higher water absorption, suggest that these wavelengths are better suited than 1,300 nm for imaging early/shallow demineralization on tooth surfaces.

Keywords

near-IR imaging; caries detection; dentistry

*Corresponding to: Cynthia Lee Darling, Department of Preventive and Restorative Dental Sciences, University of California, San Francisco, 707 Parnassus Avenue, San Francisco, CA 94143. cynthia.darling@ucsf.edu.

Conflict of Interest Disclosures: All authors have completed and submitted the ICMJE Form for Disclosure of Potential Conflicts of Interest and have disclosed the following: [none of the authors have potential conflicts of interest that need to be disclosed].

INTRODUCTION

The caries process is potentially preventable and curable. If carious lesions are detected early enough, it is likely that they can be arrested/reversed by non-surgical means through fluoride therapy, antibacterial therapy, dietary changes, or by low intensity laser irradiation [1,2]. Therefore, one cannot overstate the importance of detecting lesions in the early stage of development at which point non-invasive preventive measures can be taken to halt further decay. New imaging methods that provide improved contrast between sound and demineralized enamel will increase the clinician's ability to detect early caries lesions, assess the efficacy of intervention and identify high caries risk.

Optical imaging methods used for caries detection exploit either directly or indirectly (fluorescence) the increased light scattering in enamel caused by demineralization. Early enamel white spot lesions can be discriminated from sound enamel by visual observation or by visible-light diffuse reflectance imaging [3,4]. Very early lesions can be detected visually, and color in addition to the intensity of the reflected light plays a large role in detecting those changes. However, such color changes are difficult to quantify, and the color of sound tooth structure varies markedly. Specular reflectance is also a problem since enamel has a high refractive index. However, the visibility of scattering structures on highly reflective surfaces such as teeth can be enhanced by use of crossed polarizers to remove the glare from the surface [5,6]. The contrast between sound and demineralized enamel can be further enhanced by depolarization of the scattered light in the area of demineralized enamel [7,8]. A more difficult problem to overcome is visible light absorption due to stains. In a recent study of natural lesions in the occlusal surfaces of extracted teeth, the image contrast was actually negative as opposed to being positive in visible reflectance measurements indicating that absorption due to stains contributed more than increased scattering due to demineralization to the reflectivity in the visible [9]. Therefore, it is difficult to use visible imaging methods in areas subject to heavy staining, namely the areas where most lesions are likely to develop. Visible light reflectance methods were introduced two decades ago for use in monitoring early demineralization on tooth surfaces but were not well received [4].

Laser-induced fluorescence or quantitative light fluorescence (QLF) has been used extensively to quantify the severity of incipient caries lesions [10–17] and aid in early detection. One major advantage of fluorescence is that it removes interference from specular reflection; since the light detected is at a different wavelength to the incident light. QLF measures the loss of the enamel native fluorescence as the lesion increases in severity [18]. The pores in the lesion, formed due to demineralization, scatter and attenuate fluorescence that originates from the underlying sound enamel and dentin. The fluorescence loss (%) has been compared with the mineral loss integrated with depth, ΔZ (Vol.% mineral*μm) to give a measure of the lesion severity. However, stains prove to be a problem with fluorescence imaging methods since they both absorb visible light and contain fluorophores that fluoresce in the visible. Therefore, reliable measurements require very clean surfaces and this may be very difficult to achieve in the pits and fissures of the occlusal surface.

Near-infrared (near-IR) reflectance measurements yield high contrast for both artificial and natural caries lesions without interference from stains and color variations since none of the

known chromophores absorb light in the near-IR beyond 1,300 nm. In a previous study by Wu et al. [19], we compared the image contrast of artificial lesions produced on tooth buccal and occlusal surfaces between fluorescence, visible reflectance, near-IR reflectance, and near-IR transillumination at 1,300 nm. In that study near-IR reflectance (1,300 nm) yielded the highest contrast, although it did not break statistically with fluorescence, it was significantly higher than visible reflectance. Near-IR transillumination did not work well because the highly scattering dentin masked the shallow enamel lesions. In that study, we had used 470 nm excitation and it has been suggested that better performance can be achieved with 405 nm excitation. The fluorescence emission spectra and quantum yields are expected to be independent of excitation wavelength, according to Kasha's law as long as there is sufficient energy to populate the excited state [20]. However, light scattering and absorption in enamel varies markedly with wavelength which may influence fluorescence excitation. A study by Endo et al. [21] was consistent with Kasha's law, they measured demineralization using two QLF systems operating at 488 and 370 nm and reported similar performance. However, more recent studies by Zhang et al. [22] suggest performance differences with varying excitation wavelengths. Therefore, for this study we chose the excitation wavelength of 405 nm to be consistent with existing clinical systems and the best reported diagnostic performance.

More recent near-IR imaging studies suggest that near-IR wavelengths coincident with areas of higher water absorption are well suited for the detection of early demineralization on tooth surfaces. We hypothesize that higher water absorption in the underlying dentin and enamel reduces the reflectivity in sound areas and this in turn results in higher contrast between sound and demineralized enamel. Hyperspectral reflectance measurements by Zakian show that the tooth appears darker with increasing wavelength [23]. A recent study by Chung et al. [9] of natural occlusal lesions indicated that other near-IR wavelengths with higher water absorption yielded significantly higher contrast in reflectance than for 1,300 nm and in the visible.

Light scattering in sound dental enamel decreases markedly in the near-IR region and studies have shown that enamel has the highest transparency near 1,300 nm [24,25]. At this wavelength, the attenuation coefficient is only 2–3 cm^{-1}, which is a factor of 20–30 times lower than in the visible region [25]. At longer wavelengths, water absorption increases significantly and reduces the penetration of the near-IR light. Even though the light scattering for sound enamel is at a minimum in the near-IR, the light scattering coefficient of enamel increases by two to three order of magnitude upon demineralization due to the formation of pores on a similar size scale to the wavelength of the light that act as Mie scatterers [26]. Therefore, caries lesions can be imaged with high contrast at 1,300 nm [8]. These seminal studies established the feasibility of acquiring high-quality images of natural caries lesions using near-IR transillumination. However, those imaging geometries are not well suited for imaging early lesions that are confined to the outer enamel surface and a previous study by Wu et al. [19] indicated that the contrast of early lesions was indeed low in transillumination.

The purpose of this study is to compare QLF (405/500), visible reflectance and reflectance at three near-IR wavelengths 1,300, 1,460, and 1,600 nm for imaging early lesions on

occlusal surfaces. The study design is very similar to that carried out by Wu et al. [19], however, in this study the aim is to show that near-IR reflectance measurements at wavelengths with high water absorption yield higher contrast than conventional methods and near-IR reflectance at 1,300 nm. In addition, we employed 405 nm excitation for QLF which is similar to the systems commercially available.

MATERIALS AND METHODS

Samples and Lesion Preparation

Twenty-four human teeth with non-carious occlusal surfaces were collected (CHR approved) and sterilized with gamma radiation. Tooth occlusal surfaces were abraded using air abrasion with 50-μm glass beads for 20 seconds to remove all the stain and debris from the fissures and remove the outermost fluoride rich layers of enamel to facilitate the demineralization of those surfaces. Next, teeth were mounted in black orthodontic acrylic blocks. Samples were stored in a moist environment of 0.1% thymol to maintain tissue hydration and prevent bacterial growth. The outlines of two 4 × 4 mm windows approximately 50-μm deep were cut on the occlusal surface of each tooth using a CO_2 laser (Impact 2500, GSI Lumonics Rugby, UK) operating at a wavelength of 9.3-μm, pulse duration of 15-microseconds and a pulse repetition rate of 5 Hz. A water spray was used, and the incident fluence was 170 J/cm^2 with a spot size of 150-μm. The laser incisions also inhibit decay in the laser area due to thermal modification of the enamel and are therefore very effective in providing a separation between the sound and demineralized areas. The channels cut by the laser also serve as reference points for optical coherence tomography and for serial sectioning and are sufficiently narrow that they do not interfere with calculations of the image contrast. The enamel surrounding the 4 × 4 mm windows created by the laser was covered with red fingernail polish (Revlon, New York, NY). The varnish was removed using acetone after the lesions were generated. We chose not to use a clear varnish as was done in an earlier study [19] because it is difficult to ensure complete coverage over irregular tooth surfaces. Artificial lesions were created within the 4 × 4 mm windows by immersing each tooth into a 50 ml aliquot of a Ca/PO_4/acetate solution containing 2.0 mmol/L calcium, 2.0 mmol/L phosphate, and 0.075 mol/L acetate maintained at pH 4.5 and a temperature of 37°C for either 24 and 48 hours. This method produces two groups with 12 teeth in each group with 1- and 2-day lesions, respectively, and this well proven model produces subsurface lesions approximately 50–150 μm deep with intact surfaces [27–31]. In Figure 1, depth composition 2D images taken with a Keyence VHX-1000 digital microscope (Keyence America, Elmwood Peak, NJ) are shown for both artificial lesion groups. This new type of microscope allows acquisition of either high depth of field images similar to scanning electron microscopy or 3D images of the surface tomography and is well suited for imaging tooth occlusal surfaces.

Visible and Near-IR Cross-Polarization Images

In Figure 2, the schematic for the near-IR reflectance imaging is shown. In order to acquire reflected light images, near-IR light was directed towards the occlusal surface through a broadband fused silica beamsplitter (1,200–1,600 nm) Model BSW12 (Thorlabs, Newton, NJ) and the reflected light from the tooth was transmitted by the beamsplitter to the imaging

camera. Crossed polarizers were placed after the light source and before the detector and used to remove specular reflection (glare) that interferes with measurements of the lesion contrast. The near-IR reflectance images were captured using a high resolution, high sensitivity InGaAs Camera (Model GA1280J) with a 1,280 × 1,024 pixel format, and a 15 μm pixel pitch.

In reflectance, the demineralized regions appear lighter than the sound enamel because the demineralized enamel scatters the light increasing the amount of light scattered/ reflected back towards the camera. In order to acquire visible light images, an Ocean Optics fiber-coupled tungsten-halogen lamp (Model HL-2000-FHSA) with a DFK 31AF03 FireWire camera equipped with an Infinimite lens (Infinity Photo-Optical, Boulder, CO) was used and the images were captured using a CCD camera. A beamsplitter was not used and illumination was directed at the occlusal surface with a 5° angle from the surface normal, A and B of Figure 2 rotated by 85° towards the camera D. Crossed polarizers were also used to reduce specular reflection for the visible light reflectance measurements.

Fluorescence Loss Measurements

To collect fluorescence images, a GaN laser diode module “Blu-Ray” (λ = 405 nm) operating with 60-mW (Photonic Products, Salem, NH) was used as an excitation source. A 500 nm long-pass filter #C47-616 (Edmund Scientific, Barrington, NJ) and a DFK 31AF03 FireWire camera (The Imaging Source, Charlotte, NC) with a 1,024 × 768 element sensor equipped with a Infinimite lens (Infinity Photo-optical, Boulder, CO), were used to image the fluorescence from the surface at wavelengths longer than 500 nm. Imaging was carried out in the dark to avoid the interference of ambient light. The same illumination scheme used for visible reflectance was used without a beamsplitter. QLF systems have been employed using several excitation wavelengths ranging from 370 to 488 nm and we chose the excitation wavelength of 405 nm to be consistent with clinical systems and the best reported diagnostic performance. QLF-fluorescence loss measurements are typically reported as a ratio in intensity (fluorescence radiance) of the lesion area compared with an equivalent sound area on the tooth. We used the more traditional approach of reporting the linear image contrast which is less susceptible to errors caused by major variations in the tooth topography between the sound or reference area and the lesion area or window. Line-profiles across the sound and demineralized areas were used to calculate the ratio of intensity between the sound and demineralized regions. However, either method should yield similar results.

Image Analysis

Line profiles were extracted at the same position from the most severe area of each image across each 4 × 4 mm window and lesion or image contrast was calculated using the equation $(I_S - I_L)/I_S$; where I_S is the mean intensity of the sound enamel outside the window area, and I_L is the mean intensity of the lesion inside the window for fluorescence measurements. The intensity was averaged from an area of 25 × 25 pixels along the line profile inside and outside the lesion area. Reflectance and visible measurements $(I_L - I_S)/I_L$ have the reverse contrast that is the intensity in lesion areas is higher than for the sound enamel. The image contrast varies from 0 to 1 with 1 being very high contrast and 0 no

contrast. All image analysis was carried out using Igor pro software (Wavemetrics, Inc., Lake Oswego, OR). A one-way analysis of variance (ANOVA) followed by the Tukey–Kramer *post hoc* multiple comparison test was used to compare groups for each type of lesion employing Prism software (GraphPad, San Diego, CA).

Polarization Sensitive Optical Coherence Tomography (PS-OCT System)

PS-OCT was used as a surrogate for histology since several studies have demonstrated that it can accurately measure the depth and severity of early lesions on both smooth and occlusal tooth surfaces [28,30–32]. An all-fiber-based optical coherence domain reflectometry system was used with polarization maintaining optical fiber, high-speed piezoelectric fiber-stretchers and two balanced InGaAs receivers that was designed and fabricated by Optiphase, Inc. (Van Nuys, CA). This two-channel system was integrated with a broadband superluminescent diode (SLD) Denselight (Jessup, MD) and a high-speed XY-scanning system (ESP 300 controller and 850G-HS stages, National Instruments, Austin, TX) for *in vitro* optical tomography. This system is based on a polarization-sensitive Michelson white light interferometer. The high power (15 mW) polarized SLD source operated at a center wavelength of 1,317 nm with a spectral bandwidth full-width at half-maximum (FWHM) of 84 nm was aligned using polarization controller to deliver 15 mW into the slow axis of the PM fiber of the source arm of the interferometer. This light was split into the reference and sample arms of the Michelson interferometer by a 50/50 PM-fiber coupler. The sample arm was coupled to an AR-coated fiber-collimator to produce a 6-mm in diameter, collimated beam. That beam was focused onto the sample surface using a 20-mm focal length AR-coated planoconvex lens. This configuration provided lateral resolution of approximately 20 μm and an axial resolution of 10 μm in air with a signal to noise ratio of greater than 40–50 dB. The PS-OCT system is completely controlled using Labview software (National Instruments). The system is described in greater detail in reference [6]. Acquired scans are compiled into *b-scan* files. Image processing was carried out using Igor Pro, data analysis software (Wavemetrics, Inc.). The lesion depth and integrated reflectivity were calculated using automated image analysis routines as described previously [30,31].

RESULTS

The higher resolution and improved size of the new InGaAs sensor provides more detailed images of the occlusal images and aids in visualizing variations in the lesion severity and the complex topography of the occlusal surface. Examples of each image for two samples are shown in Figures 3 and 4. In reflectance, the lesions should appear lighter (positive contrast) than the surrounding sound enamel and in fluorescence they should appear darker (fluorescence loss). Variation in the lesion severity appears to be more pronounced in the near-IR reflectance images versus visible reflectance and fluorescence. In Figure 3, there is a distinct area of more severe demineralization which stands out with higher contrast than the surrounding lesion areas in Figures 3A–C. In the visible, however, Figure 3D, the structure is less visible and the lesion appears much more uniform. The structure is not visible at all in the fluorescence image, Figure 3E. The lesion should appear as a darker structure. Figure 3 is also interesting because it contains part of a natural lesion just outside the 4 × 4 mm

window in a small fissure indicated by the arrow in Figure 3A. Since this lies outside the 4 × 4 mm window the stained lesion was not initially removed by air abrasion. Note how the area has very high contrast in the near-IR reflectance images, Figure 3A–C, but it appears with negative contrast in the visible, Figure 3D, that is appears darker, due to stain in the fissure which dominates the contrast. It also appears with high contrast in the fluorescence image of Figure 3E.

PS-OCT measurements served as a surrogate for histology. Measurements were carried out to nondestructively assess the depth and severity of the lesions on all the samples. The mean integrated reflectivity in units of ΔR (dB × μm) was 911 ± 343 for 1-day lesion areas with an average depth of 177 ± 40 μm on the occlusal surface and 1,244 ± 320 for 2-day lesion areas with an average depth of 215 ± 55 μm. Four teeth, two from each group were sectioned and examined using polarized light microscopy and the lesion depths in those samples was consistent with the depths determined using PS-OCT.

Figure 5 shows a 2D image of the reflectivity integrated over the lesion depth for the same tooth shown in Figure 4, calculated from cross-polarization optical coherence tomography for each point in the image. The integrated reflectivity was calculated by identifying the tooth surface and the depth of the lesion at each point in the image using automated image analysis and edge detection algorithms described previously [30,31] and then integrating the reflectivity over that depth. The whiter values indicate higher integrated reflectivity and greater lesion severity. The higher reflectivity areas in the near-IR images correspond well with the areas of greater lesion severity shown in the cross-polarization PS-OCT image.

The mean ± SEM contrast values for the 1- and 2-day occlusal lesions for the various imaging methods are plotted in Figures 6 and 7 and tabulated in Table 1. Repeated measures ANOVA with Tukey–Kramer *post hoc* test was used to compare the sample groups. The highest contrast values were for the 1,460 and 1,600 nm reflectance measurements. The contrast was significantly higher than for the other imaging wavelengths and imaging modalities for all the lesions. QLF (405/500) was significantly higher than for near-IR reflectance and visible reflectance.

DISCUSSION

Near-IR reflectance measurements at 1,460 and 1,600 nm yielded the highest lesion contrast, and that contrast was significantly higher at those wavelengths than it was for the 1,300 nm reflectance measurements, fluorescence and for the visible reflectance measurements.

Examination of the sample windows using optical coherence tomography and polarized light microscopy show that the demineralization is not uniform and that the lesion depth and severity exhibits considerable variation across each window. The appearance of the lesions exhibits considerable variation with imaging wavelength and modality. Even though the lesions are not uniform, they appear quite uniform in the visible light reflectance images while they exhibit considerable variability in the near-IR reflectance images. This observation can be explained by the recent reflectance measurements and Monte Carlo simulations of photon propagation of Zhang et al. [33] that show that shorter wavelengths

yield higher contrast for very shallow demineralization and that longer wavelengths yield higher contrast for deeper lesions. Namely, the lesion contrast does not increase as much for shorter wavelengths as it does for longer wavelengths as the lesion depth and severity increases; therefore, the lesions appear more uniform in the visible than they do in the near-IR. The fluorescence images show more variation across the lesion area than the visible reflectance images but do not show as much variation as the near-IR images. A large variation in the lesion contrast with lesion severity may be advantageous for estimating the depth and severity from a single image. More extensive studies over a greater range of lesion severity are required to determine the optimum performance ranges for each of these imaging methods.

The purpose of this study is to show the potential of near-IR reflectance imaging for imaging shallow demineralization on tooth occlusal surfaces, namely lesions less than a few hundred microns deep. However, other approaches have been proposed for imaging deeper penetrating lesions. Zakian et al. [23] have employed three near-IR wavelengths to estimate the lesion severity for deeply penetrating natural occlusal lesions. Another approach for deeply penetrating lesions is to combine both near-IR reflectance and near-IR transillumination measurements. Since shallow lesions manifest high contrast in reflectance and low contrast in transillumination, one approach is to acquire reflectance and transillumination images and use both to gauge severity. For example, superficial hypomineralization does not appear darker on near-IR transillumination images while the more severe caries lesions do [34].

In this study, the lesion contrast was significantly higher for fluorescence than it was for 1,300 nm reflectance and visible light reflectance. This contradicted the results of the prior study of Wu et al. [19] in which the contrast was higher at 1,300 nm versus fluorescence. In that prior study, 470 nm excitation was employed as opposed to 405 nm excitation and there may be superior performance for the shorter excitation wavelength. However, the lesion contrast for 1,300 nm reflectance was lower than it was in that previous study [19]. If the image contrast in the near-IR were particularly sensitive to the lesion severity than we would expect large differences in performance. The performance of both the visible reflectance and the fluorescence appeared better in this study. The approach of bead blasting the occlusal surface to aid lesion development and remove stains may have enhanced the contrast for visible light reflectance and fluorescence. This was not done in the study of Wu et al. [19].

This study clearly demonstrates that a near-IR imaging system has considerable potential for the imaging of early surface demineralization with high contrast on both occlusal surfaces. The near-IR wavelengths coincident with higher water absorption yielded significantly higher contrast than other methods. The high contrast between sound enamel and early enamel demineralization suggest that reflective near-IR imaging may be effective for routine monitoring white spot lesions during chemical intervention. Since near-IR wavelengths are safe, the dentist can acquire multiple near-IR images of the lesions during subsequent visits to determine if fluoride therapy is effective in arresting the lesion or whether the lesion has expanded, requiring more aggressive intervention. Such an approach is not practical with radiographic methods due to repeated X-ray exposure.

The ability to remove the influence of stain and discoloration by imaging at near-IR wavelengths is a very significant advantage that should not be underestimated and it is probably of greater value than higher contrast. It is important to stress the fact that the occlusal surfaces were bead blasted to remove all stain and debris and that it is not feasible to carry out such a vigorous cleaning procedure clinically. In this study, the lesion contrast was positive and quite high for visible reflectance; however, the profound effect of stains may render visible light reflectance impractical as was shown in a prior study on natural lesions [9].

CONCLUSION

The results of this study suggest that near-IR reflectance measurements at longer near-IR wavelengths coincident with higher water absorption yield higher contrast of early caries lesions than other near-IR and visible wavelengths. Therefore, we anticipate improved performance for near-IR reflectance imaging systems operating at 1,460 and 1,600 nm over 1,300 nm and we are using these wavelengths for *in vivo* near-IR reflectance imaging studies of caries lesions.

Acknowledgments

Contract grant sponsor: NIH/NIDCR; Grant number: R01-DE14698

The authors would like to thank Michal Staninec and Jacob Simon for their help with this study.

References

1. NIH. Diagnosis and management of dental caries throughout life: NIH Consensus Statement. 2001 Mar 26–28.:1–24. Report no. 18.
2. Featherstone JDB. Prevention and reversal of dental caries: Role of low level fluoride. Community Dent Oral Epidemiol. 1999; 27:31–40. [PubMed: 10086924]
3. Angmar-Mansson B, ten Bosch JJ. Optical methods for the detection and quantification of caries. Adv Dent Res. 1987; 1(1):14–20. [PubMed: 3481546]
4. ten Bosch JJ, van der Mei HC, Borsboom PCF. Optical monitor of in vitro caries. Caries Res. 1984; 18:540–547. [PubMed: 6593126]
5. Benson PE, Ali Shah A, Robert Willmot D. Polarized versus nonpolarized digital images for the measurement of demineralization surrounding orthodontic brackets. Angle Orthod. 2008; 78(2): 288–293. [PubMed: 18251618]
6. Everett, MJ.; Colston, BW.; Sathyam, US.; Silva, LBD.; Fried, D.; Featherstone, JDB. Non-invasive diagnosis of early caries with polarization sensitive optical coherence tomography (PS-OCT). Lasers in dentistry V; San Jose. 1999; SPIE; p. 177-183.
7. Fried D, Xie J, Shafi S, Featherstone JDB, Breunig T, Lee CQ. Early detection of dental caries and lesion progression with polarization sensitive optical coherence tomography. J Biomed Opt. 2002; 7(4):618–627. [PubMed: 12421130]
8. Fried, D.; Featherstone, JDB.; Darling, CL.; Jones, RS.; Ngaotheppitak, P.; Buehler, CM. Early caries imaging and monitoring with near-IR light. In: Boston, DW., editor. Clinical models workshop: Remindemin, precavitation, caries. Philadelphia: W. B Saunders Company; 2005. p. 771-794.
9. Chung S, Fried D, Staninec M, Darling CL. Multispectral near-IR reflectance and transillumination imaging of teeth. Biomed Opt Express. 2011; 2(10):2804–2814. [PubMed: 22025986]

10. Ando M, Hall AF, Eckert GJ, Schemehorn BR, Analoui M, Stookey GK. Relative ability of laser fluorescence techniques to quantitate early mineral loss in vitro. Caries Res. 1997; 31(2):125–131. [PubMed: 9118184]
11. Hafstroem-Bjoerkman U, de Josselin de Jong E, Oliveby A, Angmar-Mansson B. Comparison of laser fluorescence and longitudinal microradiography for quantitative assessment of *in vitro* enamel caries. Caries Res. 1992; 26:241–247. [PubMed: 1423438]
12. Angmar-Masson, BA.; Al-Khateeb, S.; Tranaeus, S. Intraoral use of quantitative light-induced fluorescence detection method. Early detection of dental caries; Indianapolis; 1996; Indiana University, Indiana University, Indiana Conference; p. 39-50.
13. Lagerweij MD, van der Veen MH, Ando M, Lukantsova L. The validity and repeatability of three light-induced fluorescence systems: An in vitro study. Caries Res. 1999; 33:220–226. [PubMed: 10207198]
14. Eggertsson H, Analoui M, Veen MHvd, Gonzalez-Cabezas C, Eckert GJ, Stookey GK. Detection of early interproximal caries in vitro using laser fluorescence, dye-enhanced laser fluorescence and direct visual examination. Caries Res. 1999; 33:227–233. [PubMed: 10207199]
15. de Josselin de Jong E, Sundstrom F, Westerling H, Tranaeus S, ten Bosch JJ, Angmar-Mansson B. A new method for in vivo quantification of changes in initial enamel caries with laser fluorescence. Caries Res. 1995; 29(1):2–7. [PubMed: 7867045]
16. van der Veen, MH.; de Josselin de Jong, E.; Al-Kateeb, S. Caries activity detection by dehydration with qualitative light fluorescence. Early detection of dental caries II; Indianapolis, IN. 1999; Indiana University, Indiana Conference; p. 251-260.
17. Stookey, GK. Quantitative light fluorescence: A technology for early monitoring of the caries process. In: Boston, DW., editor. Clinical models workshop: Remindemin, precavitation, caries. Philadelphia: W. B Saunders Company; 2005. p. 753-770.
18. ten Bosch, JJ. Summary of research of quantitative light fluorescence. Early detection of dental caries II; Indianapolis, IN. 1999; Indiana University, Indiana Conference; p. 261-278.
19. Wu J, Fried D. High contrast near-infrared polarized reflectance images of demineralization on tooth buccal and occlusal surfaces at λ = 1310-nm. Lasers Surg Med. 2009; 41(3):208–213. [PubMed: 19291753]
20. Lakowicz, JR. Principles of fluorescence spectroscopy. New York: Kluwer Academic; 1999.
21. Ando, M.; Analoui, M.; Schemehorn, BR.; Stookey, GK. Comparison of light-induced and laser-induced fluorescence methods for the detection and quantification of enamel demineralization. Lasers in Dentistry V; San Jose. 1999; SPIE; p. 148-153.
22. Zhang L, Nelson LY, Seibel EJ. Red-shifted fluorescence of sound dental hard tissue. J Biomed Opt. 2011; 16(7):071411. [PubMed: 21806257]
23. Zakian C, Pretty I, Ellwood R. Near-infrared hyperspectral imaging of teeth for dental caries detection. J Biomed Opt. 2009; 14(6):064047. [PubMed: 20059285]
24. Fried D, Featherstone JDB, Glena RE, Seka W. The nature of light scattering in dental enamel and dentin at visible and near-IR wavelengths. Appl Opt. 1995; 34(7):1278–1285. [PubMed: 21037659]
25. Jones, RS.; Fried, D. Attenuation of 1310-nm and 1550-nm laser light through sound dental enamel. Lasers in dentistry VIII; San Jose. 2002; SPIE; p. 187-190.
26. Darling CL, Huynh GD, Fried D. Light scattering properties of natural and artificially demineralized dental enamel at 1310-nm. J Biomed Opt. 2006; 11(3):034023.
27. Featherstone JDB, Glena R, Shariati M, Shields CP. Dependence of *in vitro* demineralization and remineralization of dental enamel on fluoride concentration. J Dent Res. 1990; 69:620–625. [PubMed: 2312892]
28. Jones RS, Darling CL, Featherstone JD, Fried D. Imaging artificial caries on the occlusal surfaces with polarization-sensitive optical coherence tomography. Caries Res. 2006; 40(2):81–89. [PubMed: 16508263]
29. Jones RS, Fried D. Remineralization of enamel caries can decrease optical reflectivity. J Dent Res. 2006; 85(9):804–808. [PubMed: 16931861]

30. Kang H, Jiao JJ, Lee C, Le MH, Darling CL, Fried D. Nondestructive assessment of early tooth demineralization using cross-polarization optical coherence tomography. IEEE J Sel Top Quantum Electron. 2010; 16(4):870–876. [PubMed: 21660217]

31. Le MH, Darling CL, Fried D. Automated analysis of lesion depth and integrated reflectivity in PS-OCT scans of tooth demineralization. Lasers Surg Med. 2010; 42(1):62–68. [PubMed: 20077486]

32. Fried D, Xie J, Shafi S, Featherstone JD, Breunig TM, Le C. Imaging caries lesions and lesion progression with polarization sensitive optical coherence tomography. J Biomed Opt. 2002; 7(4): 618–627. [PubMed: 12421130]

33. Zhang L, Nelson LY, Seibel EJ. Spectrally enhanced imaging of occlusal surfaces and artificial shallow enamel erosions with a scanning fiber endoscope. J Biomed Opt. 2012; 17(7):076019. [PubMed: 22894502]

34. Hirasuna K, Fried D, Darling CL. Near-IR imaging of developmental defects in dental enamel. J Biomed Opt. 2008; 13(4):044011. [PubMed: 19021339]

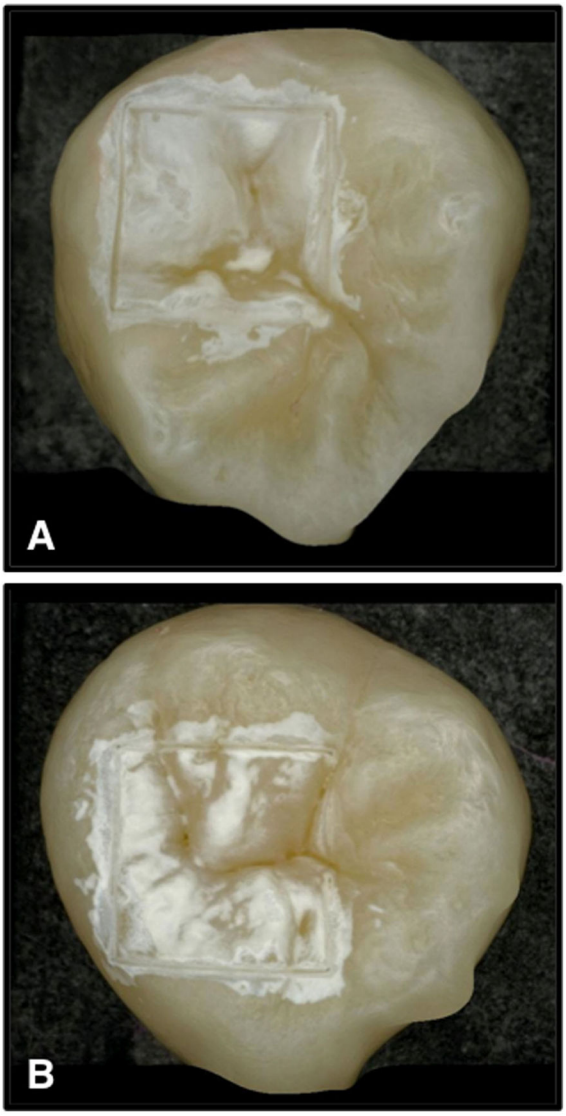

Fig. 1.
Depth composition 2D images of 1-day (top) and 2-day (bottom) lesions using Keyence VHX-1000E digital microscope (Itasca, IL).

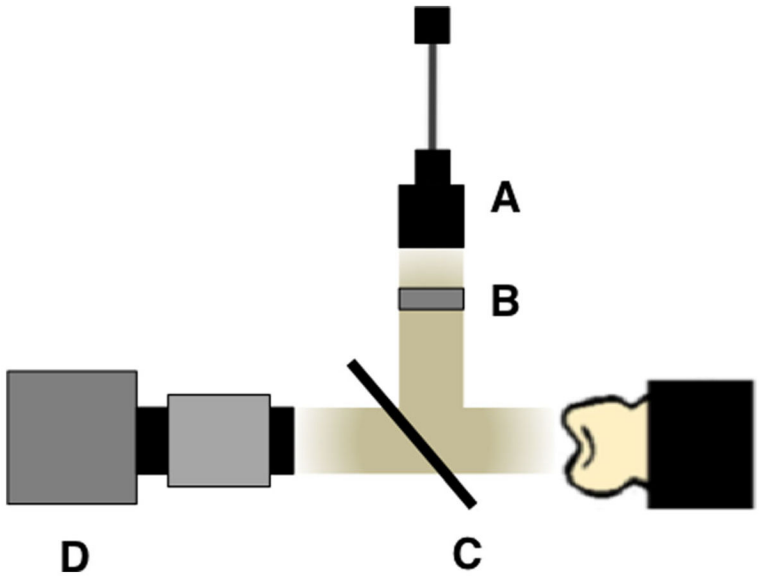

Fig. 2.

Schematic diagram for near-IR reflectance imaging: (**A**) 1,300, 1,460, and 1,600 mm SLD light source, (**B**) near-IR linear polarizer, (**C**) beamsplitter, and (**D**) UTC Aerospace Systems (GA1280J) High-resolution InGaAS SWIR Camera (1,280 × 1,024 pixel format, 12.5 mm pitch) (Princeton, NJ).

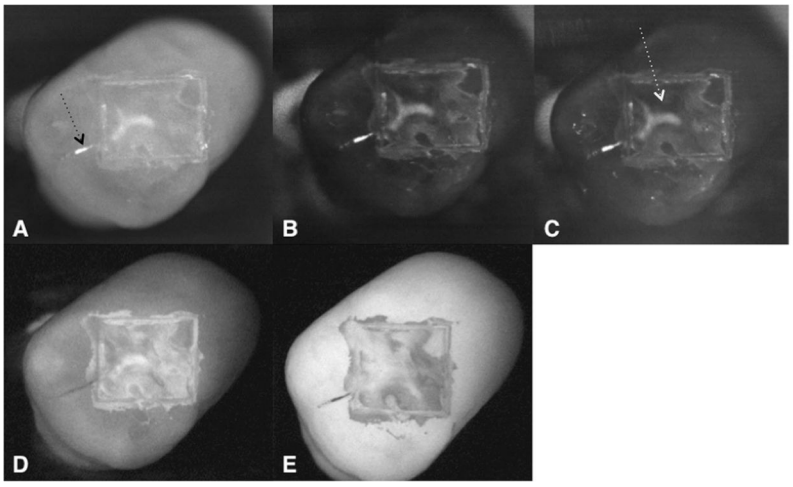

Fig. 3.

Occlusal images of 1-day lesions are shown for one sample: near-IR reflectance images w/ crossed polarizer's, (**A**) 1,300 nm, (**B**) 1,460 nm, and (**C**) 1,600 nm, along with (**D**) visible reflectance image w/crossed polarizers and (**E**) fluorescence image. Note the high contrast area of more severe demineralization in the near-IR images (white arrow in [**C**]) along with the residual natural demineralization and stain outside the 4 × 4 mm window (black arrow in [**A**]).

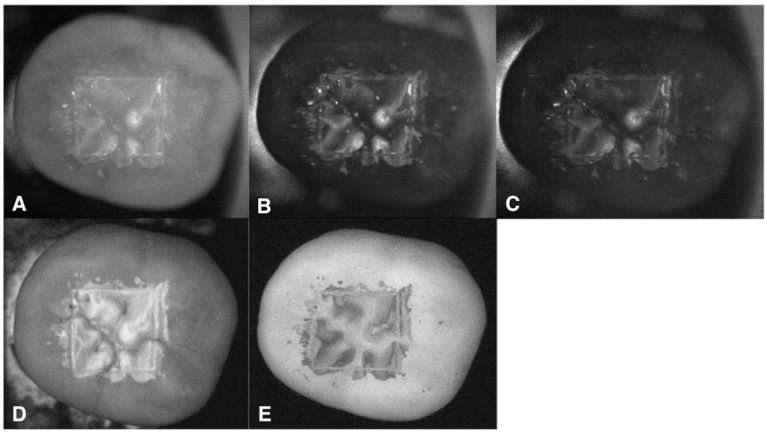

Fig. 4.

Occlusal images of 2-day lesions are shown for one sample: near-IR reflectance images w/ crossed polarizer's (**A**) 1,300 nm, (**B**) 1,460 nm, and (**C**) 1,600 nm, along with (**D**) visible reflectance image w/crossed polarizers and (**E**) fluorescence image.

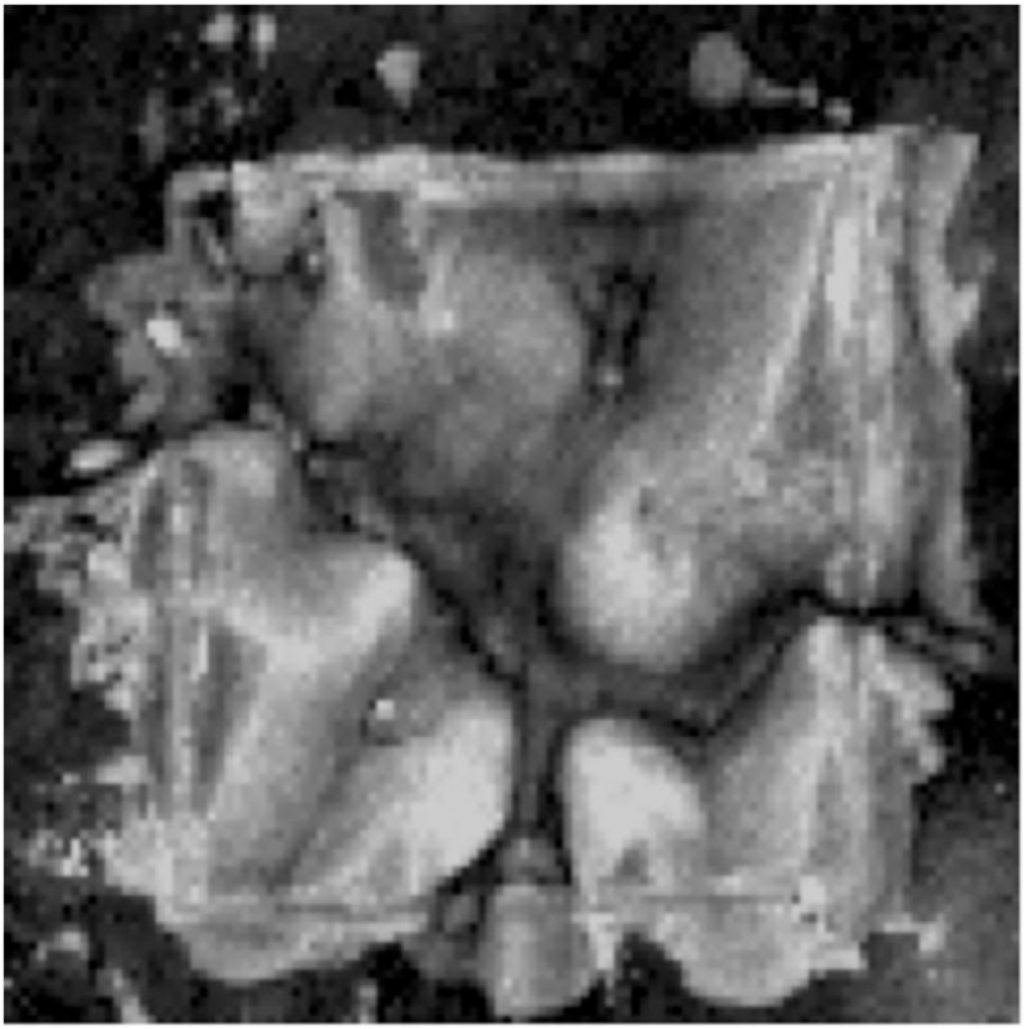

Fig. 5.

Image of the integrated reflectivity calculated from the PS-OCT image for the same tooth shown in Figure 4. Whiter areas are indicative of a high-integrated reflectivity with lesion depth, representing more severe demineralization, while black represents areas of less demineralization, image is 125 × 107 pixels.

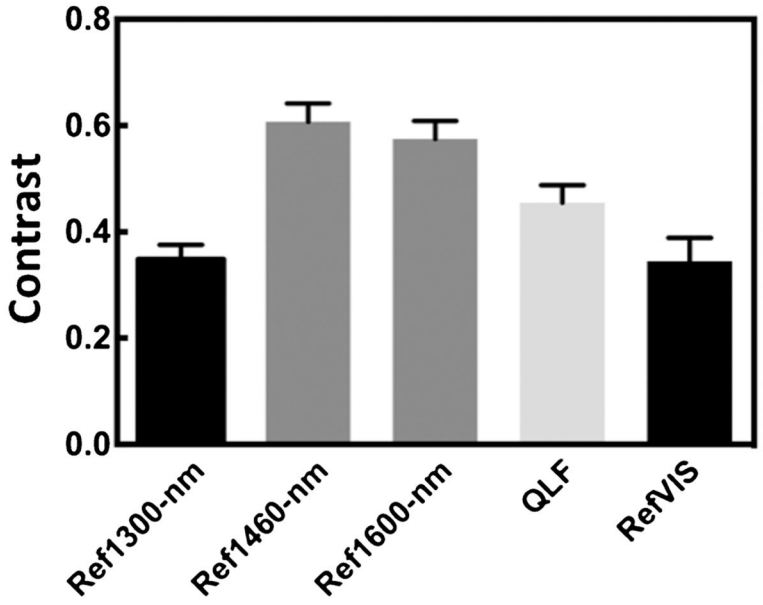

Fig. 6.

The mean ± SEM contrast values of 1-day occlusal lesions for the various imaging methods. Bars containing the same color are not significantly different ($P > 0.05$).

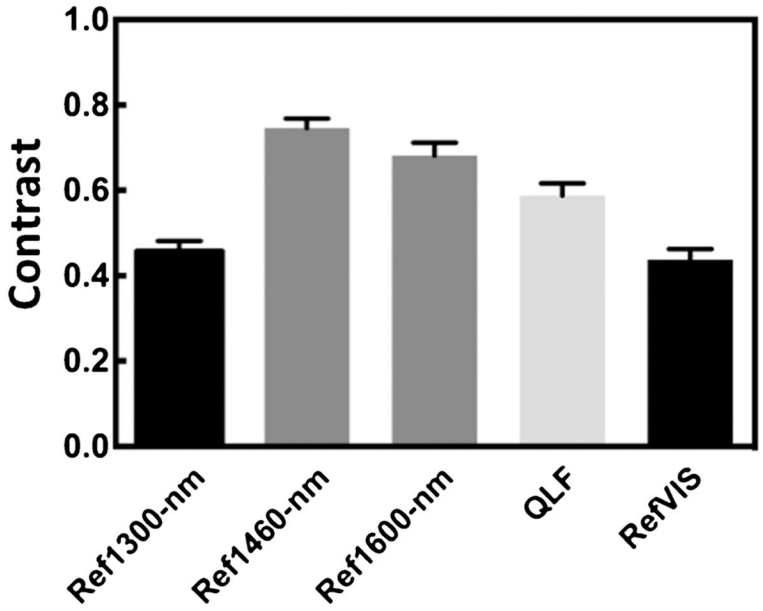

Fig. 7.

The mean ± SEM contrast values of 2-day occlusal lesions for the various imaging methods. Bars containing the same color are not significantly different ($P > 0.05$).

TABLE 1

Mean ± SEM Contrast Values of 1- and 2-Day Occlusal Lesions for Near-IR Reflectance, Visible, and Fluorescence Imaging Methods

Experiment	1-Day	*	2-Day	*
Near-IR reflectance 1,300 nm	0.35 (0.03)	a	0.46 (0.02)	c
Near-IR reflectance 1,460 nm	0.61 (0.03)	b	0.75 (0.02)	d
Near-IR reflectance 1,600 nm	0.57 (0.03)	b	0.68 (0.03)	d
Visible reflectance	0.34 (0.04)	a	0.44 (0.03)	c
Fluorescence (405/500)	0.45 (0.03)		0.59 (0.03)	

* Groups containing the same letter in each column are statistically similar ($P > 0.05$).